Effects of Pd on Catalysis by Au: CO Adsorption, CO Oxidation, and Cyclohexene Hydrogenation by Supported Au and Pd–Au Catalysts

Timothy Ward,[†,§] Laurent Delannoy,[‡] Ruth Hahn,[†,⊥] Shane Kendell,[†,∥] Christopher J. Pursell,[†] Catherine Louis,[‡] and Bert D. Chandler[†,*]

[†]Department of Chemistry, Trinity University, San Antonio, Texas 78212-7200, United States

[‡]Laboratoire de Réactivité de Surface, UMR 7197 CNRS, Université Pierre et Marie Curie-UPMC, 4 place Jussieu, 75252 Paris Cedex 05, France

ABSTRACT: Incorporating small amounts of Pd into supported Au catalysts has been shown to have beneficial effects on selective hydrogenation reactions, particularly 1,3-butadiene hydrogenation and the hydrogenation of nitro-aromatics, especially *p*-chloronitrobenzene. Appropriate Pd incorporation enhances hydrogenation activity while maintaining the desirable high selectivity of supported Au catalysts. To better understand this phenomenon, a series of alumina- and titania-supported Au and dilute Pd–Au catalysts were prepared via urea deposition–precipitation. The catalysts were studied with infrared spectroscopy of CO adsorption, CO oxidation catalysis, and cyclohexene hydrogenation catalysis

with the goal of understanding how Pd affects the catalytic properties of Au. CO adsorption experiments indicated a substantial amount of surface Pd when the catalyst was under CO. Adsorption experiments at various CO pressures were used to determine CO coverage; application of the Temkin adsorbate interaction model allowed for the determination of adsorption enthalpy metrics for CO adsorption on Au. These experiments showed that Pd induces an electronic effect on Au, affecting both the nascent adsorption enthalpy (ΔH_0) and the change in enthalpy with increasing coverage. This electronic modification had little effect on CO oxidation catalysis. Michaelis–Menten kinetics parameters showed essentially the same oxygen reactivity on all the catalysts; the primary differences were in the number of active sites. The bimetallic catalysts were poor cyclohexene hydrogenation catalysts, indicating that there is relatively little exposed Pd when the catalyst is under hydrogen. The results, which are discussed in the context of the literature, indicate that a combination of surface composition and Pd-induced electronic effects on Au appear to increase hydrogen chemisorption and hydrogenation activity while largely maintaining the selectivities associated with catalysis by Au.

KEYWORDS: IR spectroscopy, Pd–Au catalyst, CO heat of adsorption, cyclohexene hydrogenation, Temkin adsorption, CO oxidation, selective hydrogenation
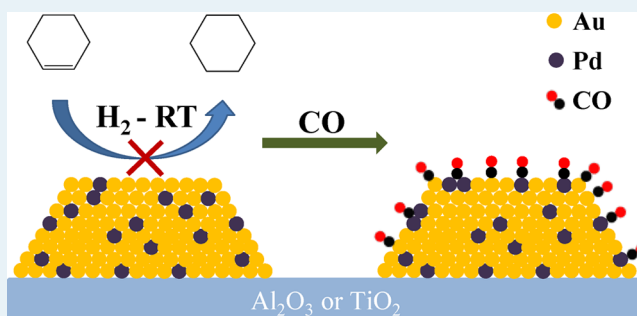
INTRODUCTION

The high activity of supported gold nanoparticles for catalyzing CO oxidation at subambient temperatures has been well documented over the past 20 years.[1,2] The last several years have seen intense interest in applying Au catalysts to a variety of other reactions,[3,4] including the water-gas shift reaction,[5–7] acetylene hydrochlorination,[8] addition of nucleophiles to acetylenes,[9] alcohol oxidation to acids and aldehydes,[10,11] and direct formation of hydrogen peroxide.[12] Selective hydrogenation reactions have also been examined, particularly for nitroaromatic compounds,[13,14] 1,3-butadiene,[15] and acetylene.[16,17] In most cases, gold catalysts have highly desirable selectivities, but activities are generally lower than classic hydrogenation metals (e.g., Pt, Pd, Ni).

One means of increasing activity and selectivity is to dope the primary component with a second metal. In the particular case of Au-containing catalysts, supported Pd–Au catalysts have been, by far, the most widely studied. This is largely due to

their use as industrial catalysts in vinyl acetate monomer synthesis,[18–20] although there is also recent interest in employing Pd–Au catalysts in the direct formation of hydrogen peroxide.[21,22] Interestingly, the functional catalysts appear to be quite different for these two reactions. In vinyl acetate monomer synthesis, the most active and selective catalyst appears to be a fairly dilute arrangement of Pd atoms in a largely Au surface, despite Au/Pd atomic ratios close to 1.[18–20] Conversely, direct hydrogen peroxide synthesis appears to be most facile on catalysts composed of a largely Pd surface with Au in the particle interior (Au/Pd atomic ratios ≅ 0.5).[22–24]

Several other reactions have also been recently investigated over Pd–Au catalysts, including direct oxidation of primary alcohols,[25] formic acid dehydrogenation for hydrogen storage,[26]

and C–H bond activation.[27] The broad interest in these reactions has led to substantial investigations of the effects of Au on catalysis by Pd. Although Au has important catalytic properties of its own, there have been relatively few studies of the effects of heterometals on catalysis by Au. In the bulk, Au is largely immiscible with most transition metals (Pd, Cu, and Ag are the notable exceptions), so well-defined alloys have been difficult to prepare, even at the nanoscale. The Pd–Au system therefore provides important opportunities to begin to understand the effects of heterometals on Au catalysis.

Recently, Keane and co-workers studied selective hydrogenation of p-chloronitrobenzene over a series of Au and Pd–Au catalysts prepared by deposition–precipitation.[14] They found that properly prepared dilute Pd/Au nanoparticles (less than 10 mol % Pd) increased hydrogenation activity several fold while maintaining nearly 100% selectivity for chloroaniline, the desired product. The particle sizes of the catalysts were all similar, so differences in activity could not be attributed to different dispersions. Louis and co-workers followed this study by examining 1,3-butadiene selective hydrogenation and found similar results: small amounts of Pd present in bimetallic particles resulted in increased hydrogenation activity while maintaining the high selectivity associated with monometallic Au catalysts.[28,29] They also found substantially enhanced hydrogen chemisorption on the bimetallic catalysts. Hutchings and co-workers studied acetylene hydrochlorination over dilute Pd–Au catalysts prepared by coimpregnation and found increased activity when adding small amounts of Pd.[30] However, they also observed a significant loss in reaction selectivity.

In the current study, we further examine this system with an eye toward understanding the enhanced hydrogenation activity of dilute Pd–Au bimetallic catalysts prepared by deposition–precipitation. Specifically, we probe electronic changes to the surface Au sites by using infrared spectroscopy to measure CO adsorption isotherms on Au. Applying a Temkin adsorption model yields coverage-dependent heat of adsorption values that are related to Pd-induced electronic changes to the surface Au atoms. CO oxidation reaction metrics are also used to evaluate the effects of electronic changes on this reaction, and cyclohexene hydrogenation is used as a probe reaction to evaluate Pd surface concentrations under hydrogenation conditions.

EXPERIMENTAL SECTION

Materials and Reagents. Water was purified to a resistivity of 17–18 MΩ-cm with a Barnstead Nanopure system. All gases were Praxair or Air Products 5.0 grade cylinders and used without further purification. The 5% CO/He mixture was purchased in an aluminum cylinder to avoid potential contamination by iron carbonyls. Titanium mesh (30 × 30 with a 0.003 in. diameter) was purchased from Unique Wire Weaving Co. and used in IR spectroscopy experiments.

The Au, Pd, and Pd–Au catalysts were prepared on Al_2O_3 and TiO_2 via urea deposition–precipitation of $HAuCl_4$ and $PdCl_2$ according to previously published procedures.[14,28] Au and Pd–Au catalysts with Au/Pd ratios of 20:1 and 10:1 were prepared with a nominal Au loading of 1 wt %. The Pd sample contained 300 ppm Pd, which corresponds to the Pd loading in Pd–Au with a ratio of 20:1 ratio. The deposited precursors were reduced under flowing H_2 at 300 °C for 2.5 h (heating rate 3 °C/min), as previously described.[14,28] The samples were

then transferred to 1 dram screw-cap vials and stored in a desiccator.

Elemental Analysis via ICP-OES. The Au content was determined using a Varian 720-ES inductively coupled plasma optical emission spectrometer (ICP-OES). Approximately 25 mg of catalyst was accurately weighed in a beaker. Freshly prepared aqua regia (6 mL) was then added to the sample and allowed to digest at room temperature for 30 min. The sample was then heated slowly to 60 °C for 2 h, and the resulting solution was filtered into a 25 mL volumetric flask. The sample was diluted to mark with water and subsequently analyzed. Experimental errors for the method and the spectrometer are typically <5%.

Infrared Spectroscopy of Adsorbed CO. Infrared spectroscopy experiments were performed as previously reported.[31,32] Approximately 25 mg of catalyst was pressed into a 30 × 30 Ti mesh (Unique Wire Weaving Co.). The resulting mesh-supported pellet was placed in an oven and heated in air overnight at 100 °C. After cooling, the mesh-supported pellet was mounted into a home-built copper cell and vacuum chamber with a gas-phase optical path length of 1 cm. The entire vacuum chamber was placed in the sample compartment of a Nicolet Magna 550 FT-IR spectrometer and evacuated to a pressure of $<10^{-3}$ Torr for 15 min. All measurements were made at 297 K, and all spectra were referenced to a background spectrum of the catalyst pellet under vacuum prior to the addition of CO. Transmission spectra consisted of 50 scans collected with 8 cm^{-1} resolution (spectral data spacing = 4 cm^{-1}) and were reported in absorbance units.

The gas handling system consisted of a mechanical and diffusion pump, a glass line with stainless steel transfer lines to the sample apparatus, and a Baratron pressure gauge ($P = 0$–20 Torr). A liquid nitrogen trap was used to trap out any impurities from the CO tank (UHP grade, from Air Products). The entire gas handling system was rinsed with CO three times before exposing the sample. After collecting a background spectrum, the sample was exposed to CO (roughly 20 Torr CO), and the surface was allowed to equilibrate for 5–10 min; previous work has shown that this is ample time for CO equilibration on Au catalysts.[31,32] An infrared spectrum was recorded, and the pressure in the cell was slowly decreased to the next pressure. After completing an experiment, the sample was evacuated, and the experiment was repeated for a total of two or three adsorption isotherm measurements on a single catalyst sample in a single day. To isolate the Au–CO band for the bimetallic samples, spectra were reprocessed by subtracting the lowest pressure spectrum, which included a nearly saturated Pd–CO peak.

CO Oxidation Catalysis. The CO oxidation reactor system consisted of a previously described home-built, laboratory scale, single-pass, plug-flow microreactor.[33] Feed and catalyst effluent CO, CO_2, and O_2 compositions were determined using Siemens Ultramat 23 infrared gas analyzer. Supported catalyst samples (about 10 mg) were diluted with ~1 g of 400 mesh silicon carbide (Aldrich) and placed in the microreactor. All reactions were performed at ambient pressure with 1% CO in the feed, which was maintained with Porter mass flow controllers. Previously reduced catalysts were pretreated with 10% H_2/10% O_2/80% N_2 (120 mL min^{-1}) for an hour at 250 °C. After pretreatment, the furnace was removed,. and the catalyst was allowed to equilibrate under flowing 1% CO + 20% O_2 (180 mL/min total flow, balance N_2) for 1 h. An ice or

water bath was then placed around the catalyst to control the reaction temperature. Changes in CO oxidation activity were measured as a function of temperature as well as CO and O_2 feed concentration. All activities were determined by averaging steady state conversion data for ~10 min, usually between 1 and 3 h after introducing CO to the activated catalyst. Each activity measurement was performed with a fresh catalyst sample.

Cyclohexene Hydrogenation Catalysis. The catalyst was diluted 20:1 by mass with SiC (Aldrich) and loaded into a glass U-tube. The samples were rereduced in situ, ramping the temperature 5 °C/min to 300 °C and holding for 1 h. The reactor was then cooled to the reaction temperature under flowing H_2. The cyclohexene in H_2 feed was prepared using a 2-stage bubbler. The first stage was held at ambient temperature, and the second stage was maintained at 0 °C.[34]

The reaction was monitored using an SRI 8610C gas chromatograph with automatic gas sampling valve, 1 mL sample loop, and FID detector. Products and reactants were quantified using a SiO_2 column operated at 260 °C. Peak areas were standardized against external calibration solutions of cyclohexene in hexanes and cyclohexane in cyclohexene. Cyclohexene hydrogenation rates for the Pd and Pd−Au bimetallic catalysts were measured by monitoring conversion as a function of flow rate. Flow rates were measured with a bubble flow meter immediately prior to each injection. Plots of conversion vs inverse space velocity were linear and had y-intercepts of 0.02% or lower. Due to their extremely low activity, rates for the supported Au catalysts were determined from single point experiments at each temperature. In all cases, conversions were below 5% to maintain differential reactor conditions.

■ RESULTS

Six catalysts were characterized with ICP-OES, infrared spectroscopy (CO adsorption), CO oxidation catalysis, and cyclohexene hydrogenation catalysis. Catalyst designations were based on the nominal elemental ratios. The experimental Au/Pd ratios determined by ICP are close to the values used in the synthesis (Table 1). All of the catalysts in this study have

Table 1. Elemental Analysis Data for Au and Pd−Au Catalysts

catalyst	mass % Au	mass % Pd	mole % Pd[a]	Au/Pd
Au/TiO_2	0.75			
Pd_1Au_{20}/TiO_2	0.78	0.019	4.4	22
Pd_2Au_{20}/TiO_2	0.77	0.039	8.5	11
Pd/TiO_2		0.043	100	
Au/Al_2O_3	0.71			
Pd_1Au_{20}/Al_2O_3	0.70	0.015	3.9	25
Pd_2Au_{20}/Al_2O_3	0.80	0.037	8.0	12
Pd/Al_2O_3		0.009	100	

[a]Mole percent reflects ratios of the noble metals only.

previously been characterized with transmission electron microscopy and have similar particle sizes, with average particle diameters around 2−3 nm.[14,15,28]

Infrared Spectroscopy of CO Adsorption. The bimetallic catalysts have previously shown enhanced activity and selectivity for chloronitrobenzene[14] and 1,3-butadiene hydrogenation.[28,29] To better understand the nature of the enhanced catalysis and probe possible electronic changes to the surface

Au sites, we characterized the catalysts with infrared transmission spectroscopy of adsorbed CO at room temperature. Results for CO adsorption on Au/Al_2O_3 are shown in Figure 1.
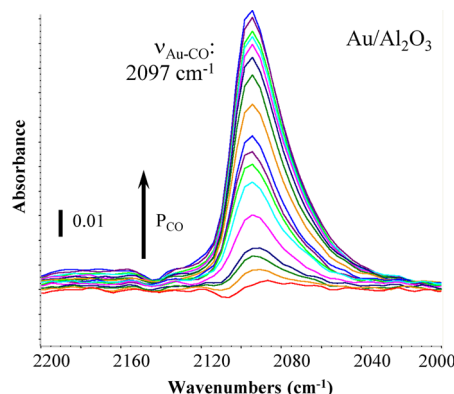

Figure 1. FT-IR spectra of CO adsorbed on the Au/Al_2O_3 catalyst.

The peak at ~2100 cm^{-1} is consistent with CO adsorption on metallic gold, as we and others have previously shown.[31,32] The monometallic Pd samples did not bind CO because of surface oxidation during air exposure and pellet drying (see the Experimental Section). In situ reduction was unavailable in our system, so we limit our analysis to the effects of Pd incorporation into Au nanoparticles.

Figures 2 and 3 show spectra for CO adsorbed on the Pd_2Au_{20}/Al_2O_3 and Pd_1Au_{20}/Al_2O_3 catalysts, respectively.
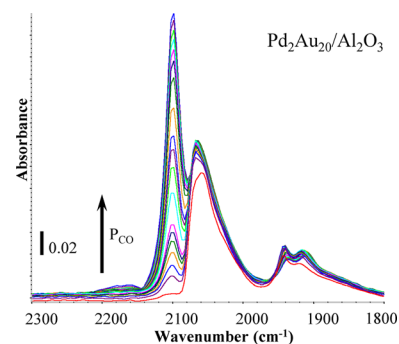
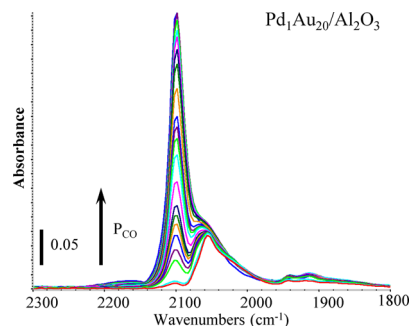**Figure 2.** FT-IR spectra of CO adsorbed on the Pd_2Au_{20}/Al_2O_3 catalyst.

Figure 3. FT-IR spectra of CO adsorbed on the Pd_1Au_{20}/Al_2O_3 catalyst.

Spectra for the titania-supported samples are similar but are omitted for brevity. Three prominent bands are present. The highest energy band, near 2100 cm^{-1}, is attributed to CO on

surface Au sites.[31,32] The peaks near 2065 and 1940 cm^{-1} are attributed to linear and bridge bonded CO on Pd, respectively.[35-37] As with the Au/Al$_2$O$_3$ sample, the Au−CO peak area changes with increasing pressure. The Pd−CO peaks, however, show very little change with pressure, indicating that the Pd sites are nearly saturated at the lowest pressure used in this study (10 mTorr).

The spectra of the bimetallic catalysts have several items of note. First, the CO adsorption experiments are performed ex-situ, so the reduced catalyst is exposed to air, and the pellet is dried at 100 °C in air prior to analysis (see the Experimental Section). Under these mild thermal conditions, the mono-metallic Pd samples undergo surface oxidation and do not adsorb CO. However, when Pd is associated with Au in the bimetallic samples, Pd oxidation does not occur, since surface Pd−CO bands are readily observed in the IR spectra. Second, there is a substantial amount of surface Pd under the conditions of the CO adsorption experiment. Third, the spectra of CO bound to the bimetallic catalysts are dominated by linearly bound Pd−CO, rather than the bridge-bonded CO that dominates the spectra for CO adsorbed on Pd nanoparticles and surfaces.[35-37] Comparing the spectra in Figures 2 and 3, the relative amount of bridging CO tracks with the amount of Pd in the sample. That is, the catalyst with more Pd has a greater fraction of bridging sites. These results are fully consistent with previously reported DRIFTS experiments.[28,29]

It is difficult to ascertain potential changes in the Au−CO stretching frequency from the raw spectra of CO adsorbed on the bimetallic catalysts. The linear Pd−CO band overlaps with part of the Au−CO band; thus, the peak maximum and peak areas include contributions from both spectral bands and must be deconvoluted. To isolate the Au−CO band, we reprocessed the spectra, subtracting the spectrum collected at the lowest CO pressure. This spectrum contains only the Pd−CO band, which is nearly saturated at 10 mTorr. The resulting spectra, plotted in Figure 4, show essentially the same CO stretching frequency as the monometallic Au samples (~2100 cm^{-1}, Figure 1); that is, there is no observed shift in the CO stretching frequency upon Pd incorporation. The reprocessed spectra also have accurate Au−CO peak areas as a function of CO pressure, which can be used to quantify CO adsorption on Au catalysts and extract thermodynamic metrics for CO binding.[32,38,39]

Details of the data analysis can be found in previous publications.[32,38] Briefly, the peak areas assigned to CO adsorbed on Au are used to determine an adsorption isotherm. The adsorption isotherm is then fit using the Temkin adsorbate interaction model.[32,38] This model invokes a linear change in the adsorption enthalpy with coverage due to Au mediated substrate−substrate interactions.

$$\Delta G_{\theta,T} = \Delta H_0 - \theta \delta \Delta H - T\Delta S \qquad (1)$$

The $\Delta G_{\theta,T}$ values can be determined analytically at individual coverages from the adsorption isotherm, allowing one to evaluate an experimentally determined ΔG as a function of coverage:

$$\Delta G_{\theta,T} = -RT \ln\left(\frac{\theta}{P(1-\theta)}\right) \qquad (2)$$

The linear portion of the data (usually corresponding to surface coverages between $\theta = 0.2$ and 0.8) and a previously determined ΔS_{ads} value (-142 J/(mol K) for titania supported
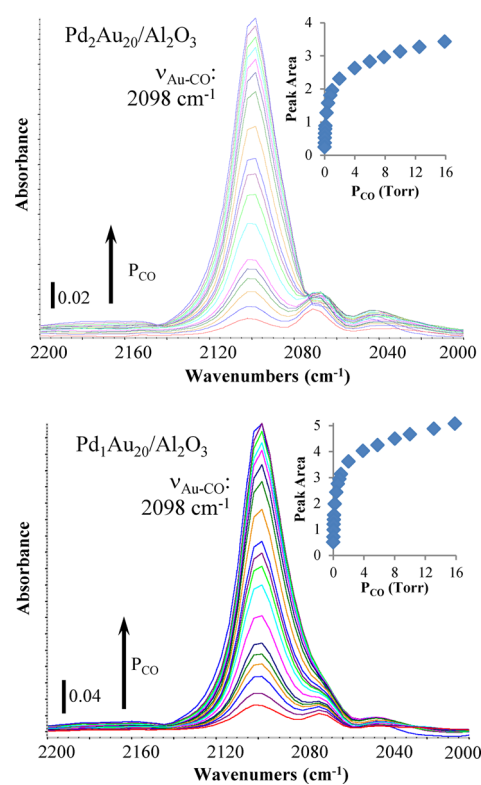

Figure 4. FT-IR spectra of CO adsorbed to Au sites on the Pd$_2$Au$_{20}$/Al$_2$O$_3$ (top panel) and Pd$_1$Au$_{20}$/Al$_2$O$_3$ (bottom panel) catalysts. The spectrum of CO bound to the Pd sites was subtracted from each of the spectra in Figures 2 and 3 to isolate the Au-bound CO.

samples and -120 J/(mol K) for alumina-supported samples) were used to extract two values that describe each catalyst.[32] The heat of CO adsorption at zero coverage (ΔH_0), which is determined from the y-intercept of the linear data, describes the nascent binding energy for CO on the catalyst when no adsorbate interactions are present. The second value, $\delta \Delta H$, describes the change in the adsorption energy from $\theta = 0$ to $\theta = 1$ (i.e., from ΔH_0 to ΔH_1) with full coverage representing saturation of the CO binding sites. The CO binding sites are some subset of the total number of surface Au sites, most likely the low coordinate corner and edge atoms.[32] In the Temkin adsorbate interaction model, this change in adsorption enthalpy is attributed to electronic interactions between the CO adsorbates and the Au nanoparticles and thus, describes, how the surface electronic properties change with coverage.[32,38]

Representative Temkin plots for the catalysts are shown in Figure 5; the extracted ΔH_0 and $\delta \Delta H$ values are compiled in Table 2. The data indicate that Pd incorporation into the catalyst results in a moderate electronic modification of the Au nanoparticles that results in changes to the Au−CO bond strength. The alumina-supported bimetallic catalysts show a 1.5−3 kJ/mol increase in ΔH_0, indicating stronger CO binding at low coverage. At the same time, $\delta \Delta H$ doubles relative to the Au/Al$_2$O$_3$ sample. The results on the titania-supported catalysts show a similar electronic effect, although the changes in both ΔH_0 and $\delta \Delta H$ relative to Au/TiO$_2$ are attenuated.

CO Oxidation Catalysis. The catalysts were also examined with CO oxidation catalysis, collecting activity, apparent activation energy, and oxygen dependence data. The mono-metallic Pd samples were completely inactive for CO oxidation under these conditions, and the apparent activation energy and
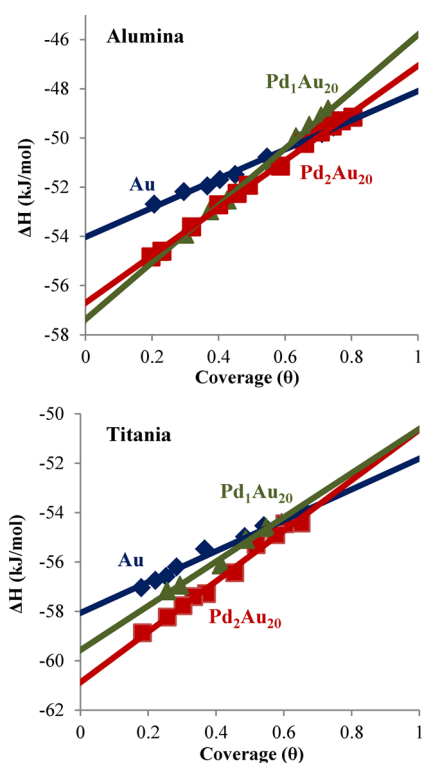
Figure 5. Temkin plots for the alumina- (top panel) and titania-supported (bottom panel) catalysts.

Table 2. Thermodynamic Metrics for CO Adsorption

catalyst	$-\Delta H_0$ (kJ/mol)	$-\delta \Delta H$ (kJ/mol)
Au/Al_2O_3	54.3 ± 0.7	5 ± 2
Pd_1Au_{20}/Al_2O_3	57.8 ± 0.4	12 ± 2
Pd_2Au_{20}/Al_2O_3	56.1 ± 0.1	10 ± 1
Au/TiO_2	58.1 ± 0.2	7 ± 2
Pd_1Au_{20}/TiO_2	59.4 ± 1.8	10 ± 1
Pd_2Au_{20}/TiO_2	59.6 ± 0.1	10 ± 2

oxygen reaction order data for Au/TiO_2 and Au/Al_2O_3 (shown in Table 3) are consistent with our previous observations for supported Au catalysts.[33,39,40] Higher reaction temperatures are required to observe CO conversion over the alumina-supported

**Table 3. CO Oxidation Activity Data for Au and Pd−Au Catalysts**

catalyst	rate[a] (1/s)	Temp (°C)	E_{app} (kJ/mol)	O_2 rxn order	ν_{max} (1/s)	K_R (atm)
Au/TiO_2	0.19	−1	27.7	0.42	0.28	0.06
Pd_1Au_{20}/TiO_2	0.28	−1	27.0	0.35	0.40	0.09
Pd_2Au_{20}/TiO_2	0.23	−1	29.2	0.35	0.28	0.08
Au/Al_2O_3	0.16	24	31.0	0.44	0.26	0.12
Pd_1Au_{20}/Al_2O_3	0.05	24	28.5	0.38	0.06	0.08
Pd_2Au_{20}/Al_2O_3	0.08	24	33.2	0.42	0.13	0.11

[a] $P(O_2)$ = 0.2 atm, average of 2 runs on 2 different samples. Rates are expressed as mole of CO converted per total mole Au per second. Note that the TiO_2 samples are more active because their kinetics were determined at a lower temperature.

catalysts, indicating that the titania-supported catalysts are more active for CO oxidation.

The oxygen pressure data can also be evaluated with double reciprocal plots using a Michaelis−Menten type treatment.[33] This treatment is used to provide a means of extracting quantitative parameters that describe O_2 reactivity for individual gold catalysts; it is not intended to capture all of the molecular complexity of every elementary step in the reaction mechanism. A full derivation of this treatment has been previously published.[33] Briefly, a simple characterization mechanism (Scheme 1), which has also been suggested by DFT calculations,,[41,42] is used to describe the reaction.

Scheme 1
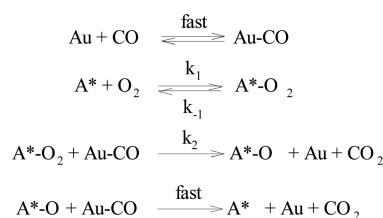
The characterization mechanism in Scheme 1 is intentionally nonspecific regarding the nature of the active site for O_2 activation. Structurally, it requires only that O_2 is bound and activated someplace on the catalyst close to a Au surface atom capable of binding CO. Beyond this, the characterization mechanism requires no further assumptions regarding the nature or structure of the active site. The assumption that oxygen is bound at or near a Au−CO site is widely agreed upon in the literature, although debate remains regarding the nature and structure of the active site.[1,2,43] One of the goals of this work is to glean some insight into how Pd might affect the number and nature of active sites; it is therefore prudent to make as few structural and kinetic assumptions about the active site(s) as possible.

In the key kinetic steps of the characterization mechanism, oxygen is bound at an active site (A*) and then reacts with readily available CO to produce CO_2. Subsequent steps to produce a second equivalent of CO_2 and regenerate the active site are considered fast steps after the rate-determining step in this kinetic model, and are therefore kinetically unobservable. This is consistent with the widely held belief that O_2 activation is rate-determining in CO oxidation over Au.[2,44] Similarly, this mechanism is not intended to include the details of oxygen activation, as many reasonable possibilities exist for the actual rate-determining step (e.g., oxygen migration, O−O bond scission, O atom transfer to CO, etc.). The characterization mechanism is therefore an intentionally reductionist approach designed to help foster the extraction of chemically meaningful reaction metrics. It is not intended to advance specific mechanistic possibilities or make a priori assumptions regarding the nature of the active site.

Applying a typical kinetic derivation employing the steady-state approximation to Scheme 1 yields the following expression:

$$\frac{1}{\nu_{rxn}} = \frac{K_R}{\nu_{max}}\left(\frac{1}{P_{O_2}}\right) + \frac{1}{\nu_{max}} \tag{3}$$

where ν_{rxn} is the measured reaction rate, and

$$\nu_{max} = k_2 \theta_{CO}[A^*]_T \qquad (4)$$

and

$$K_R = \frac{k_{-1} + k_2 \theta_{CO}}{k_1} \qquad (5)$$

We note that a similar set of equations can be derived using a Langmuir–Hinshelwood mechanism, although this requires some additional assumptions.[33] In eqs 3 and 5, θ_{CO} designates the coverage of the CO binding sites, which are a subset of the total Au surface sites, and $[A^*]_T$ is the total number of active sites. The total number of active sites is also assumed to involve a subset of the total number of surface Au sites. K_R and ν_{max} are descriptive kinetic parameters comparable to those employed in enzyme kinetics.[45] Analogous to the Michaelis–Menten constant, K_R is a measure of the reactivity or instability of adsorbed O_2 (cf. A^*–O_2). Similarly, ν_{max} depends both on the intrinsic reaction barrier and the number of active sites. This kinetic treatment has been previously published and has been shown to well describe kinetic data for CO oxidation over several Au[33] and bimetallic NiAu catalysts,[40] as well as a series of NaBr-poisoned Au catalysts.[39]

The activity data shown in Figure 6 and Table 3 indicate that Pd incorporation has little impact on CO oxidation rates. The
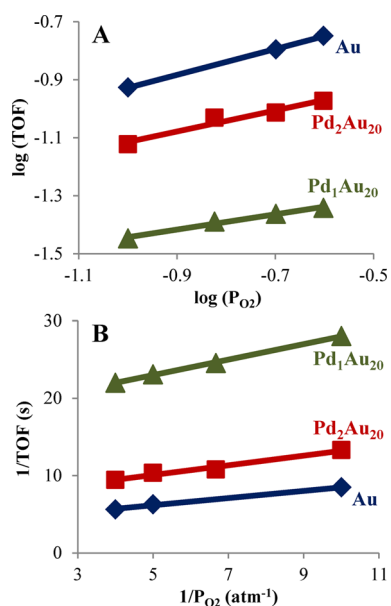

Figure 6. Kinetics plots for CO oxidation catalysis over the alumina supported catalysts: (A) O_2 reaction order and (B) double reciprocal plots used to determine K_R and ν_{max}.

O_2 reaction orders, apparent activation energies (E_{app}), and K_R values are potentially the most sensitive parameters to electronic modification of the catalyst. However, all of these parameters are essentially unaffected by Pd incorporation, indicating that the presence of Pd does not substantially affect the reactivity of gold in CO oxidation catalysis. In particular, the K_R values, which provide a semiquantitative measure of each catalyst's ability to activate oxygen, are relatively consistent for the catalysts. For comparison, bimetallic Ni–Au catalysts showed up to a 40-fold increase in K_R, albeit Ni/Au ratios >1 were required for substantial modification of the reaction kinetics.[40] For these dilute PdAu catalysts, it does not appear

that the electronic effects observed in the CO adsorption experiments are sufficient to modify CO oxidation catalysis.

It may also be possible that Pd is oxidized under the reaction conditions, changing the electronic interactions; however, as mentioned above, the Pd in the PdAu catalysts seem to be more resistant to oxidation in air at room temperature than monometallic Pd. Unfortunately, the low Pd content of the samples makes this extremely difficult to verify. Because the K_R values are consistent, the changes in ν_{max} suggest that the differences in CO oxidation catalysis are primarily due to differences in the number of active sites from one catalyst to the next. All of the catalysts have been previously characterized and found to have particle sizes in the 2–3 nm range;[14,28,29] however, the particle sizes are not strictly identical, which can result in differences in the number of active sites. Further, the number of active sites is closely tied to the in situ production of surface carbonates during the reaction which can poison the metal–support interface.[46]

Cyclohexene Hydrogenation. Supported gold catalysts are notoriously poor alkene hydrogenation catalysts, evidenced by investigations into their potential as catalysts for the selective hydrogenation of alkynes or alkadienes to alkenes.[14,16,17] Palladium, on the other hand, is an excellent alkene hydrogenation catalyst; consequently, alkene hydrogenation reactions provide a method for probing catalyst surface compositions under hydrogenation reaction conditions.[47] Catalysts with surface compositions that are largely Au are expected to behave similarly to monometallic Au, whereas catalysts that have substantial amounts of Pd on the surface are expected to have reactivity similar to Pd. Cyclohexene hydrogenation activity data are presented in Table 4. Because

Table 4. Cyclohexene Hydrogenation Activity Data for Au and Pd–Au Catalysts

catalyst	temp (°C)	rate[a] (1/min)	catalyst	temp (°C)	rate[a] (1/min)
Au/TiO_2	275	<1	Au/Al_2O_3	275	<1
Pd_1Au_{20}/TiO_2	98	2.3	Pd_1Au_{20}/Al_2O_3	98	4.0
Pd_2Au_{20}/TiO_2	98	2.8	Pd_2Au_{20}/Al_2O_3	98	19
Pd/TiO_2	11	8.4	Pd/Al_2O_3	28	180
Pd/TiO_2	20	19			
Pd/TiO_2	23	26	Pd/TiO_2	98	~5400[b]

[a]Rate expressed in moles cyclohexane per mole metal per minute. [b]Estimated from Arrhenius plot.

catalyst activity varied dramatically with composition, we were unable to evaluate all of the catalysts at a single temperature. As expected from previous studies, the monometallic Au catalysts were exceptionally poor alkene hydrogenation catalysts, showing no activity until nearly 300 °C.[15,47] The monometallic Pd catalysts were highly active, and the bimetallic PdAu catalysts begin to show activity around 100 °C, intermediate between the two monometallic catalysts.

■ DISCUSSION

The Au and Pd–Au catalysts in this study have previously been characterized with transmission electron microscopy; all of the catalysts were found to have similar particle sizes (2–3 nm).[14,15,28] The differences in the total metal surface area are therefore relatively small and cannot explain the large differences in 1,3-butadiene[28] and p-chloronitrobenzene[14] hydrogenation activity between the Au and Pd–Au catalysts.

Our study used CO adsorption, CO oxidation, and cyclohexene hydrogenation to probe the surface of the metal nanoparticles and to provide additional insight into the bimetallic catalysts. The key question that we would like to understand is: Why does Pd incorporation increase selective hydrogenation activity while largely maintaining the selectivity associated with monometallic Au catalysts?

To frame the discussion that follows, we offer two limiting cases that might explain these results and highlight the merits and shortcomings of each model. The first possibility is that Pd is present on the surface of the bimetallic nanoparticles and that this surface Pd activates H_2 more efficiently than Au. For clarity, we will refer to this as the "surface Pd" model. Since hydrogen dissociation has been suggested to be the rate-determining step in butadiene hydrogenation over Au,[15] the higher rates might be explained by the presence of this surface Pd. The second possible explanation is that incorporating Pd into Au particles induces some electronic change to the surface Au atoms and that the modified Au surface catalyzes the reaction more quickly than the monometallic Au catalysts. We will refer to this limiting case as the "electronic modification" model.

We consider the "electronic modification" model first. This explanation is attractive because the CO heat of adsorption experiments show that an electronic influence of Pd on Au does, indeed, exist: incorporating Pd into the catalyst causes a marked change in the metrics for the heat of adsorption of CO on Au (Table 2). Similar electronic effects (net electron donation from Pd to Au) have been reported by several research groups.[48−52] Baber, Tierney, and Sykes used a variety of STM techniques to show that both surface and subsurface Pd atoms were depleted of charge in Pd/Au(111) near surface alloys.[48] Williams, Monnier, and co-workers collected XPS data on Pd−Au catalysts prepared via electroless deposition; their data also suggested net electron transfer from Pd to Au.[49,50] On the basis of XPS and XANES data, Marx and Baiker concluded that the Au 5d density of states showed greater filling and shifted toward the Fermi level upon the formation of Pd−Au nanoparticles.[51] They were able to more conclusively attribute these changes to alloying with Pd by showing that the magnitude of changes in the bimetallic nanoparticles was much greater than changes associated with particle size effects or differing metal−support interactions.[51] Zhang, Li, and co-workers also used changes in the stretching frequency of CO adsorbed onto surface Pd atoms to suggest charge transfer from Pd to Au.[52]

The CO heat of adsorption data reported here are consistent with these findings from the literature. The heat of adsorption of other adsorbates, including hydrogen, is expected to scale with CO heat of adsorption.[41,53,54] The observation of increased H_2 chemisorption (higher H/metal ratios) measured on the bimetallic catalysts[14] is therefore also consistent with the electronic effect. Since hydrogen activation has been suggested to be the rate-determining step in Au-catalyzed hydrogenations,[15] this model is attractive because it provides a straightforward explanation for why the selectivity associated with Au is maintained while activity is increased upon Pd incorporation. Namely, surface Au atoms are the active sites in both the mono- and bimetallic catalysts.

The "surface Pd" model suggests that the incorporated Pd is present on the catalyst surface and functions to help activate H_2 and increase the hydrogen coverage during hydrogenation reactions. Although the CO adsorption data show an electronic effect of Pd on the Au sites, the spectra include a substantial

contribution from Pd−CO interactions (Figures 2 and 3). This provides the strongest evidence for the role of the "surface Pd" model in explaining the enhanced 1,3-butadiene hydrogenation activity. Pd is well-known to be a far superior hydrogenation catalyst, so even very small amounts of surface Pd might increase the hydrogenation activity relative to Au. The IR data also indicate that as Pd becomes more and more dilute in Au, the surface Pd atoms have a greater propensity to become isolated from one another on the surface, appearing as surface monomers.[55−57]

This data must be considered carefully, however. Comparing the CO band intensities is difficult because extinction coefficients depend on surface roughness, the angle of the vibrating dipole from the surface normal, and distance-dependent dipole coupling effects.[58−60] Further, these effects are metal-dependent. For example, Vannice and Wang found that, for CO adsorbed on Pt, higher frequency linear modes have higher extinction coefficients than do lower frequency bridging modes.[61] Vannice and Wang also reported that the opposite was true for Pd.[62] It is therefore difficult to make a quantitative evaluation of the surface composition on the basis of the IR intensities. Nevertheless, the trend as the catalyst Pd content decreases is the important observation. As the nanoparticles and surfaces become more dilute in Pd, the Pd is more likely to be found as isolated monomers surrounded by Au. At very dilute limits, one would expect there to be few if any Pd dimers on the nanoparticle surface; this has been observed by several researchers for the PdAu system.[36,63,64] Therefore, the "surface Pd" model provides a good potential explanation for the increased hydrogenation activity, but the relative influence of surface Pd dimers is unclear, particularly their role in affecting reaction selectivity.

Ultimately, the relative influence of these two models depends on the surface composition under hydrogenation conditions. We therefore consider the possibility that the surface may be substantially different under CO and hydrogen atmospheres. Goodman's group used low-energy ion scattering spectroscopy (LEIS) to show that Pd−Au alloy films are thermodynamically driven to form stable alloys with surfaces that are highly enriched in Au under ultrahigh vacuum (UHV) conditions.[35] Several groups have reported that CO can induce substantial structural changes to Pd−Au nanoparticles, with the strong Pd−CO interactions providing a driving force to draw Pd to the nanoparticle surface.[28,29,65,66] Previous studies on the same catalysts as in the present study showed that the DRIFTS spectra evolved over time under CO, suggesting that the surface composition does, indeed, change to increase the number of surface Pd atoms under CO.[28]

Given the evolution of the catalyst surface under CO and the uncertainty in the kinetics of this process, it is difficult to accurately evaluate the surface composition of the catalyst under hydrogenation conditions. However, Goodman's LEIS studies,[35] which have essentially no metal-adsorbate interactions due to the UHV conditions, provide a baseline for considering the catalyst surface structure under reactive gases. Relative to CO, hydrogen has a substantially smaller heat of adsorption on Pd;[67] therefore, hydrogen likely induces a smaller perturbation to the catalyst surface composition from the Au enrichment observed in UHV studies. It is likely that the surface contains less Pd than is observed under CO and that lower surface Pd catalysts will have a greater fraction of the Pd present as monomeric surface species. The cyclohexene hydrogenation experiments were performed specifically to

evaluate the surface Pd composition; unfortunately, the results from these experiments are ultimately ambiguous.

In understanding these differences, it is important to make a clear distinction between the substrates involved in the hydrogenation reactions. To be clear, we refer to alkenes exclusively as monoalkenes, such as propylene and cyclohexene. Polyunsaturated molecules and dienes, such as 1,3-butadiene, are considered to be chemically distinct species with relatively different chemistries and affinities for the metal catalyst. For cyclohexene hydrogenation over Au, alkene binding rather than hydrogen activation or coverage appears to be rate-determining. This experimental fact is evidenced in this study: the monometallic Au catalysts described here are inactive for gas phase cyclohexene hydrogenation below 250 °C (Table 4), yet are active for butadiene hydrogenation at temperatures as low as 100 °C. We note that liquid phase cyclohexene hydrogenation over gold catalysts has been observed at lower temperatures under much higher hydrogen pressures.[68]

Palladium, on the other hand, easily binds alkenes; thus, cyclohexene hydrogenation can be used to evaluate the amount of Pd on the surface during hydrogenation conditions. Cyclohexene hydrogenation activity on the bimetallic catalysts is between the activity of the monometallic Pd and Au catalysts (Table 4). The bimetallics are substantially more active than monometallic Au, suggesting that there is some Pd on the surface. At the same time, the bimetallics are, relative to Pd, extraordinarily inactive. We have tried to measure the cyclohexene hydrogenation activity for the Pd/TiO$_2$ catalyst at 98 °C, where the Pd–Au activity is observed. Even with highly diluted samples (~1 mg of catalyst) we cannot get conversions low enough to measure a reaction rate. On the basis of a temperature study near room temperature with the Pd/TiO$_2$ catalyst, and extrapolating an Arrhenius relationship to 98 °C, the estimated Pd activity is roughly 4 orders of magnitude higher than in the bimetallic catalysts.

This allows for some qualitative comparisons between the catalysts. If all of the cyclohexene hydrogenation activity is attributed to surface Pd atoms having comparable activity to monometallic Pd, then the surface fraction of Pd in the bimetallic catalysts would be roughly one surface Pd atom for every 1000 surface Au atoms. This corresponds to approximately one surface Pd atom per nanoparticle (a 3 nm Au particle contains roughly 1000 atoms). Although there are difficulties comparing extinction coefficients for CO in the IR data, the fraction of surface Pd atoms suggested by the cyclohexene hydrogenation data is far below what we can observe by IR spectroscopy and is inconsistent with the observation of Pd dimers.

The cyclohexene hydrogenation results therefore support the conclusion that the bimetallic catalysts have substantially less surface Pd under hydrogenation conditions than when exposed to CO. This estimation, however, was predicated on a simple model in which the surface Pd in the bimetallic catalysts has activity comparable to the surface Pd in a monometallic Pd nanoparticle. The very low cyclohexene hydrogenation activity of the bimetallic catalysts suggests that the surface Pd may be somewhat less active in the bimetallic catalysts (relative to monometallic Pd catalysts). This is consistent with a net electron transfer from Pd to Au observed in the CO binding experiments.

Finally, the two models presented ("electronic modification" and "surface Pd") represent two limiting cases that explain why the bimetallic catalysts are more active hydrogenation catalysts

than monometallic Au catalysts and yet maintain the selectivity associated with Au. The reality likely lies somewhere between the two extreme models. For example, the data is consistent with a case that, under hydrogenation conditions, a small amount of surface Pd is present and serves to dramatically increase hydrogen activation rates without providing a substantial number of sites for binding other substrates. The electronic effect of the Pd on Au then may help to stabilize surface hydrogen and increase the hydrogen surface coverage, thus speeding up reaction.

The presence of small amounts of surface Pd under hydrogenation conditions is entirely consistent with the selectivity patterns observed during 1,3-butadiene hydrogenation.[28] In butadiene hydrogenation over these Pd–Au catalysts, the diene is nearly completely converted to alkenes before alkene hydrogenation begins to form alkanes.[28] Monometallic Au catalysts, on the other hand, do not bind alkenes and hydrogenate alkenes at the moderate temperatures employed in dienes' or alkynes' hydrogenation.[16,28] As in the cyclohexene hydrogenation studies reported here, the alkene hydrogenation activity of the bimetallic catalysts lies somewhere between the hydrogenation activity of the monometallic catalysts. Beyond that, it is difficult to accurately attribute how much of this effect is due to the electronic modification of Au and how much is due to the dilution of a small amount of Pd on the catalyst surface; it is likely a combination of both.

The combination of the two models is also attractive because it explains another interesting observation for the bimetallic catalysts. Monometallic Pd catalysts undergo rapid surface oxidation in ambient air, so CO adsorption experiments must be performed after in situ reduction, with oxygen being excluded. We cannot observe CO adsorption onto monometallic Pd catalysts with the IR cell used in this study, presumably because of the presence of surface PdO, which prevents CO from adsorbing on the Pd. However, the bimetallic catalysts show substantial CO adsorption on Pd, even after air contact (see Experimental). This indicates that the Au acts to protect the Pd from oxidation by atmospheric oxygen. This could be due to a combination of most of the Pd being present as subsurface Pd (consistent with the low hydrogenation rates and CO pulling Pd to the surface). An electronic influence of Au on Pd might also weaken surface Pd–O interactions, but it is difficult to envision that this would be significant enough to prevent surface Pd oxidation.

The combined models explanation is also attractive because it is consistent with the low cyclohexene hydrogenation activity of the surface Pd. Even if one attributes the cyclohexene hydrogenation entirely to a small fraction of surface Pd atoms, the activity on a per surface Pd basis is more than an order of magnitude lower than for the monometallic Pd catalyst. This suggests that the interactions with Au lower the Pd activity through a combination of the electronic interactions and the dilution in Au, which reduces the amount of contiguous Pd atoms. Further, Hwang's group has performed a number of computational studies examining the reactivity of local Pd–Au nanostructures (Pd monomers, dimers, trimmers, etc.). They have consistently concluded that isolated Pd monomers have reactivities substantially different from other Pd structures in Pd–Au alloys.[69−71] Our results are entirely consistent with their calculations and provide a reasonable explanation for the relatively low cyclohexene hydrogenation activity of these catalysts.

CONCLUSIONS

A series of alumina and titania supported Au and dilute Pd–Au catalysts were studied with infrared spectroscopy of CO adsorption, CO oxidation catalysis, and cyclohexene hydrogenation catalysis with the goal of understanding how Pd affects the catalytic properties of Au. CO adsorption experiments indicated a substantial amount of surface Pd when the catalyst was under CO. These experiments also showed that Pd induces an electronic effect on Au, as the nascent heat of adsorption increased upon Pd incorporation. In addition, Pd incorporation affected the coverage dependence of the CO adsorption enthalpy. These electronic changes had little effect on CO oxidation catalysis. The bimetallic catalysts were poor cyclohexene hydrogenation catalysts, indicating that there is relatively little exposed Pd when the catalyst is under hydrogen. These results suggest that the enhanced activity in *p*-chloronitrobenzene and 1,3-butadiene hydrogenation described in previous studies, which occurs without deleterious effects to the inherent selectivity of pure Au catalysts, arises from a combination of dilute surface Pd under hydrogenation conditions and an electronic modification of Au surface atoms by the incorporated Pd.

AUTHOR INFORMATION

Corresponding Author
*Phone: (210) 999-7557. Fax: (210) 999-7569. E-mail: Bert.chandler@trinity.edu.

Present Addresses
§(T.W.) Department of Chemistry, University of Georgia, Athens, GA 30602-2556.
⊥(R.H.) Petroleum and Geosystems Engineering Department, University of Texas at Austin, Austin, TX 78712-1585.
∥(S.K.) Department of Physical Sciences, School of Science and Mathematics, Howard Payne University, Brownwood, TX 76801.

Notes
The authors declare no competing financial interest.

ACKNOWLEDGMENTS

REFERENCES

(1) Bond, G. C.; Louis, C.; Thompson, D. T. *Catalysis by Gold*; Imperial College Press: London, 2006; Vol. *6*.
(2) Kung, M. C.; Davis, R. J.; Kung, H. H. *J. Phys. Chem. C* **2007**, *111*, 11767.
(3) Corma, A.; Garcia, H. *Chem. Soc. Rev.* **2008**, *37*, 2096.
(4) Hashmi, S. K.; Hutchings Graham, J. *Angew. Chem., Int. Ed.* **2006**, *45*, 7896.
(5) Williams, W. D.; Shekhar, M.; Lee, W.-S.; Kispersky, V.; Delgass, W. N.; Ribeiro, F. H.; Kim, S. M.; Stach, E. A.; Miller, J. T.; Allard, L. F. *J. Am. Chem. Soc.* **2010**, *132*, 14018.
(6) Boucher, M. B.; Goergen, S.; Yi, N.; Flytzani-Stephanopoulos, M. *Phys. Chem. Chem. Phys.* **2011**, *13*, 2517.
(7) Deng, W.; Carpenter, C.; Yi, N.; Flytzani-Stephanopoulos, M. *Top. Catal.* **2007**, *44*, 199.
(8) Hutchings, G. J. *J. Catal.* **1985**, *96*, 292.
(9) Teles, J. H.; Brode, S.; Chabanas, M. *Angew. Chem., Int. Ed.* **1998**, *37*, 1415.
(10) Prati, L.; Rossi, M. *J. Catal.* **1998**, *176*, 552.
(11) Abad, A.; Concepcion, P.; Corma, A.; Garcia, H. *Angew. Chem., Int. Ed.* **2005**, *44*, 4066.
(12) Landon, P.; Collier, P. J.; Papworth, A. J.; Kiely, C. J.; Hutchings, G. J. *Chem. Commun.* **2002**, 2058.
(13) Corma, A.; Serna, P. *Science* **2006**, *313*, 332.
(14) Cardenas-Lizana, F.; Gomez-Quero, S.; Hugon, A.; Delannoy, L.; Louis, C.; Keane, M. A. *J. Catal.* **2009**, *262*, 235.
(15) Hugon, A.; Delannoy, L.; Louis, C. *Gold Bull.* **2009**, *42*, 310.
(16) Jia, J.; Haraki, K.; Kondo, J. N.; Domen, K.; Tamaru, K. *J. Phys. Chem. B* **2000**, *104*, 11153.
(17) Segura, Y.; Lopez, N.; Perez-Ramirez, J. *J. Catal.* **2007**, *247*, 383.
(18) Han, Y. F.; Wang, J. H.; Kumar, D.; Yan, Z.; Goodman, D. W. *J. Catal.* **2005**, *232*, 467.
(19) Chen, M.; Kumar, D.; Yi, C.-W.; Goodman, D. W. *Science* **2005**, *310*, 291.
(20) Han, P.; Axnanda, S.; Lyubinetsky, I.; Goodman, D. W. *J. Am. Chem. Soc.* **2007**, *129*, 14355.
(21) Edwards, J. K.; Hutchings, G. J. *Angew. Chem., Int. Ed.* **2008**, *47*, 9192.
(22) Solsona, B. E.; Edwards, J. K.; Landon, P.; Carley, A. F.; Herzing, A.; Kiely, C. J.; Hutchings, G. J. *Chem. Mater.* **2006**, *18*, 2689.
(23) Edwards, J. K.; Solsona, B.; Ntainjua, N. E.; Carley, A. F.; Herzing, A. A.; Kiely, C. J.; Hutchings, G. J. *Science* **2009**, *323*, 1037.
(24) Edwards, J. K.; Solsona, B. E.; Landon, P.; Carley, A. F.; Herzing, A.; Kiely, C. J.; Hutchings, G. J. *J. Catal.* **2005**, *236*, 69.
(25) Enache, D. I.; Edwards, J. K.; Landon, P.; Solsona-Espriu, B.; Carley, A. F.; Herzing, A. A.; Watanabe, M.; Kiely, C. J.; Knight, D. W.; Hutchings, G. J. *Science* **2006**, *311*, 362.
(26) Gu, X.; Lu, Z.-H.; Jiang, H.-L.; Akita, T.; Xu, Q. *J. Am. Chem. Soc.* **2011**, *133*, 11822.
(27) Kesavan, L.; Tiruvalam, R.; Ab Rahim, M. H.; bin Saiman, M. I.; Enache, D. I.; Jenkins, R. L.; Dimitratos, N.; Lopez-Sanchez, J. A.; Taylor, S. H.; Knight, D. W.; Kiely, C. J.; Hutchings, G. J. *Science* **2011**, *331*, 195.
(28) Hugon, A.; Delannoy, L.; Krafft, J.-M.; Louis, C. *J. Phys. Chem. C* **2010**, *114*, 10823.
(29) Kolli, N. E.; Delannoy, L.; Louis, C. *J. Catal.* **2013**, *297*, 79.
(30) Conte, M.; Carley, A. F.; Attard, G.; Herzing, A. A.; Kiely, C. J.; Hutchings, G. J. *J. Catal.* **2008**, *257*, 190.
(31) Hartshorn, H.; Pursell, C. J.; Chandler, B. D. *J. Phys. Chem. C* **2009**, *113*, 10718.
(32) Pursell, C. J.; Hartshorn, H.; Ward, T.; Chandler, B. D.; Boccuzzi, F. *J. Phys. Chem. C* **2011**, *115*, 23880.
(33) Long, C. G.; Gilbertson, J. D.; Vijayaraghavan, G.; Stevenson, K. J.; Pursell, C. J.; Chandler, B. D. *J. Am. Chem. Soc.* **2008**, *130*, 10103.
(34) Beakley, L.; Yost, S.; Cheng, R.; Chandler, B. D. *Appl. Catal., A* **2005**, *292*, 124.
(35) Yi, C. W.; Luo, K.; Wei, T.; Goodman, D. W. *J. Phys. Chem. B* **2005**, *109*, 18535.
(36) Luo, K.; Wei, T.; Yi, C. W.; Axnanda, S.; Goodman, D. W. *J. Phys. Chem. B* **2005**, *109*, 23517.
(37) Gao, F.; Wang, Y.; Goodman, D. W. *J. Phys. Chem. C* **2010**, *114*, 4036.
(38) Pursell, C. J.; Chandler, B. D.; Manzoli, M.; Boccuzzi, F. *J. Phys. Chem. C* **2012**, *116*, 11117.
(39) Chandler, B. D.; Kendell, S.; Doan, H.; Korkosz, R. J.; Grabow, L. C.; Pursell, C. J. *ACS Catal.* **2012**, *2*, 684.
(40) Chandler, B. D.; Long, C. G.; Gilbertson, J. D.; Vijayaraghavan, G.; Stevenson, K. J.; Pursell, C. J. *J. Phys. Chem. C* **2010**, *114*, 11498.
(41) Falsig, H.; Hvolboek, B.; Kristensen, I. S.; Jiang, T.; Bligaard, T.; Christensen, C. H.; Norskov, J. K. *Angew. Chem., Int. Ed.* **2008**, *47*, 4835.

(42) Nørskov and coworkers have proposed a similar mechanism based on DFT calculations (Falsig, , H.; Hvolboek, , B.; Kristensen, , I. S.; Jiang, , T.; Bligaard, , T.; Christensen, , C. H.; Norskov, , J. K. *Angew. Chem. Int. Ed.*, *47*,, 4835). The primary difference between Scheme 1 and the DFT results is the Scheme 1 assumes that the reaction between surface O atoms and adsorbed CO (the last step in the scheme) is fast. The DFT study found this last reaction step to be fast for Au catalysts and further found that direct reaction between surface bound O2 and adsorbed CO was required to accurately describe Au catalysts.

(43) Widmann, D.; Behm, R. J. *Angew. Chem., Int. Ed.* **2011**, *50*, 10241.

(44) Aguilar-Guerrero, V.; Gates, B. C. *Catal. Lett.* **2009**, *130*, 108.

(45) Our first paper deriving and employing the Michaelis−Menten treatment used KI to describe O_2 reactivity. On the basis of various feedback, we have changed the name of the constant to K_R so that it is not confused with a constant designed to describe inhibition.

(46) Saavedra, J.; Powell, C.; Panthi, B.; Pursell, C.; Chandler, B. *J. Catal.* **2013**, *307*, 37.

(47) Hugon, A.; Delannoy, L.; Louis, C. *Gold Bull.* **2008**, *41*, 127.

(48) Baber, A. E.; Tierney, H. L.; Sykes, E. C. H. *ACS Nano* **2010**, *4*, 1637.

(49) Rebelli, J.; Rodriguez, A. A.; Ma, S.; Williams, C. T.; Monnier, J. R. *Catal. Today* **2011**, *160*, 170.

(50) Rebelli, J.; Detwiler, M.; Ma, S.; Williams, C. T.; Monnier, J. R. *J. Catal.* **2010**, *270*, 224.

(51) Marx, S.; Baiker, A. *J. Phys. Chem. C* **2009**, *113*, 6191.

(52) Wei, X.; Yang, X.-F.; Wang, A.-Q.; Li, L.; Liu, X.-Y.; Zhang, T.; Mou, C.-Y.; Li, J. *J. Phys. Chem. C* **2012**, *116*, 6222.

(53) Janssens, T. V. W.; Clausen, B. S.; Hvolbaek, B.; Falsig, H.; Christensen, C. H.; Bligaard, T.; Norskov, J. K. *Top. Catal.* **2007**, *44*, 15.

(54) Jiang, T.; Mowbray, D. J.; Dobrin, S.; Falsig, H.; Hvolbaek, B.; Bligaard, T.; Norskov, J. K. *J. Phys. Chem. C* **2009**, *113*, 10548.

(55) Luo, K.; Wei, T.; Yi, C. W.; Axnanda, S.; Goodman, D. W. *J. Phys. Chem. B* **2005**, *109*, 23517.

(56) Yi, C. W.; Luo, K.; Wei, T.; Goodman, D. W. *J. Phys. Chem. B* **2005**, *109*, 18535.

(57) Yuan, D. W.; Gong, X. G.; Wu, R. Q. *Phys. Rev. B* **2008**, *78*, 4.

(58) Wei, T.; Wang, J.; Goodman, D. W. *J. Phys. Chem. C* **2007**, *111*, 8781.

(59) Gao, F.; Wang, Y.; Goodman, D. W. *J. Am. Chem. Soc.* **2009**, *131*, 5734.

(60) France, J.; Hollins, P. *J. Electron Spectrosc. Relat. Phenom.* **1993**, *64−65*, 251.

(61) Vannice, M. A.; Twu, C. C. *J. Chem. Phys.* **1981**, *75*, 5944.

(62) Vannice, M. A.; Wang, S. Y. *J. Phys. Chem.* **1981**, *85*, 2543.

(63) Yuan, D.; Gong, X.; Wu, R. *Phys. Rev. B: Condens. Matter Mater. Phys.* **2008**, *78*, 035441/1.

(64) Ponec, V. *Appl. Catal., A* **2001**, *222*, 31.

(65) Gao, F.; Wang, Y.; Goodman, D. W. *J. Phys. Chem. C* **2009**, *113*, 14993.

(66) Soto-Verdugo, V.; Metiu, H. *Surf. Sci.* **2007**, *601*, 5332.

(67) Vannice, M. A.; Chou, P. *ACS Symp. Ser.* **1986**, *298*, 76.

(68) Bus, E.; Prins, R.; van, B. J. A. *Catal. Commun.* **2007**, *8*, 1397.

(69) Ham, H. C.; Hwang, G. S.; Han, J.; Nam, S. W.; Lim, T. H. *J. Phys. Chem. C* **2009**, *113*, 12943.

(70) Ham, H. C.; Hwang, G. S.; Han, J.; Nam, S. W.; Lim, T. H. *J. Phys. Chem. C* **2010**, *114*, 14922.

(71) Ham, H. C.; Stephens, J. A.; Hwang, G. S.; Han, J.; Nam, S. W.; Lim, T. H. *J. Phys. Chem. Lett.* **2012**, *3*, 566.